[10] R. E. Collin, *Field Theory of Guided Waves*. New York: McGraw-Hill, 1960, pp. 198–209.
[11] X.-H. Zhu, D.-Z. Chen, and S.-J. Wang, "Method-of-moments solution for the posts in a circular waveguide," in *IEEE MTT-S Int. Microwave Symp. Dig.* (Dallas, TX), May 8–10, 1990, pp. 693–696.
[12] Q. Ishida, S. Kaniya, and F. Takde, "A design method of polarizer using metallic posts," *Tech. Rep. Inst. Electron. and Commun. Eng. Japan*, vol. 78, no. 178, MW78-83, pp. 1–6, Sept. 24, 1978.

Numerical Analysis of Waveguide Discontinuity Problems Using the Network Model Decomposition Method

Geyi Wen

***Abstract*—This paper presents an application of the network model decomposition method to the analysis of arbitrarily shaped H- and E-plane waveguide junctions. By using the polygon discretization technique introduced in [1], the waveguide discontinuity region, which is surrounded by a metallic wall and the reference planes chosen, is first discretized; then the topological model and the corresponding network model for the waveguide discontinuity are established. In the formulation, equivalent current sources connected to the nodes on the boundary of the region have been introduced to replace the effect of the field external to the region. The field internal to the region is approximated by the nodal voltage distribution of the network model, which can then be used to determine the scattering parameters of the waveguide junction. A diakoptic algorithm for the solution of the network model has also been developed. To illustrate the applications and show the validity of the method, numerical results for various H- and E-plane junctions have been given and a favorable comparison has been made with other existing theories.**

I. Introduction

In an earlier paper, a method termed network model decomposition (NMD) was presented for the solution of transmission line problems. The object of the present paper is to describe the application of the NMD method to the analysis of scattering by H- or E-plane waveguide junctions. A topological model for the waveguide discontinuity is first established by dividing the discontinuity region into polygonal subregions; the corresponding network model is then formulated on the basis of the topological model and the field equations. In the formulation, the field internal to the waveguide discontinuity region is discretized and represented by a nodal voltage distribution. The field external to the region is replaced by equivalent current sources connected to the boundary nodes, without affecting the field distribution inside the region. A diakoptic algorithm is also developed for the solution of the network models, by means of which the computational efforts and computer core storage can be greatly reduced.

To show the validity and usefulness of the network model decomposition method, computed results are given for various H- and E-plane waveguide discontinuities. In all cases studied, the power conservation condition is satisfied to an accuracy of $\pm 10^{-5}$.

Manuscript received June 12, 1990; revised January 2, 1991.
The author is with the Institute of Applied Physics, University of Electronic Science and Technology of China, Chengdu 610054, People's Republic of China.
IEEE Log Number 9101020.

II. Topological Models and Network Models

An arbitrarily shaped n-port waveguide junction is shown in Fig. 1(a), where the reference planes Γ_p ($p = 1, 2, \cdots, n$) and the metallic wall Γ_0 completely enclose the waveguide discontinuity region Ω; d_p is the width, a_p, or the height, b_p, of the waveguide p for the H- or E-plane junction. The waveguide p is assumed to be filled with dielectric of relative permittivity ϵ_{rp}.

If the excitation by the dominant TE_{10} mode is assumed, then the waveguide discontinuity can be described by the following equations [9]:

$$\nabla^2 \varphi + \hat{K}^2 \varphi = 0 \tag{1}$$

$$\hat{K}_0^2 = K_0^2 \hat{\epsilon}_r \tag{2}$$

$$K_0^2 = \omega^2 \mu_0 \epsilon_0 \tag{3}$$

$$\hat{\epsilon}_r = \begin{cases} \epsilon_r & \text{(for } H\text{-plane junction)} \\ \epsilon_r - (\pi / K_0 a)^2 & \text{(for } E\text{-plane junction)} \end{cases} \tag{4}$$

$$\varphi = \begin{cases} E_z & \text{(for } H\text{-plane junction)} \\ H_z & \text{(for } E\text{-plane junction)} \end{cases} \tag{5}$$

where E_z and H_z are the z components of electric and magnetic field respectively.

Following the procedure described in [1], the waveguide discontinuity region is first discretized by using polygon discretization techniques (Fig. 1(b)). Then the topological model for the waveguide discontinuity problem can be established (Fig. 1(c)). The set of all the oriented branches and the incidence matrix of the topological model will be denoted by $S_b = \{b_1, b_2, \cdots, b_b\}$ and $A = \{a_{ij}\}$ respectively. Then we have the equivalent form of Kirchhoff's voltage laws as follows:

$$U_b = A^T V \tag{6}$$

where $V = (\varphi_1, \varphi_2, \cdots, \varphi_N)^T$ is the node-to-datum voltage vector; φ_k is the value of φ at node n_k ($k = 1, 2, \cdots, N$); and U_b is the branch voltage vector.

Making use of the approximation introduced in [1], the node equation for an interior node n_k can be expressed in terms of the incidence matrix A as

$$\sum_{i=1}^{e_k} a_{kl_i} Y_{k_i} u_{l_i} = \sum_{l=1}^{b} a_{kl} i_{bl} = 0 \tag{7}$$

where u_{l_i} is the branch voltage, i_{bl} the branch current and Y_{k_i} the branch admittances:

$$\begin{cases} Y_{k_0} = -\hat{K}^2 S_k \\ Y_{k_i} = \left(\overline{p_{i-1} q_i} + \overline{q_i p_i}\right) \big/ \overline{m_i n_k} \end{cases} \tag{8}$$

We now construct the node equation for a boundary node. The dual element G_k of a boundary node n_k is shown in [1, fig. 2(b)]. The following relation can then be derived in a similar way:

$$\sum_{i=2}^{e_k - 1} \int_{\overline{p_{i-1} q_i p_i}} \frac{\partial \varphi}{\partial n} d\Gamma + \int_{\overline{q_1 p_1}} \frac{\partial \varphi}{\partial n} d\Gamma + \int_{\overline{p_{e_k - 1} q_{e_k}}} \frac{\partial \varphi}{\partial n} d\Gamma + \hat{K}^2 \iint_{G_k} \varphi \, ds + \int_{\overline{n_k q_1}} \frac{\partial \varphi}{\partial n} d\Gamma + \int_{\overline{n_k q_{e_k}}} \frac{\partial \varphi}{\partial n} d\Gamma = 0. \tag{9}$$

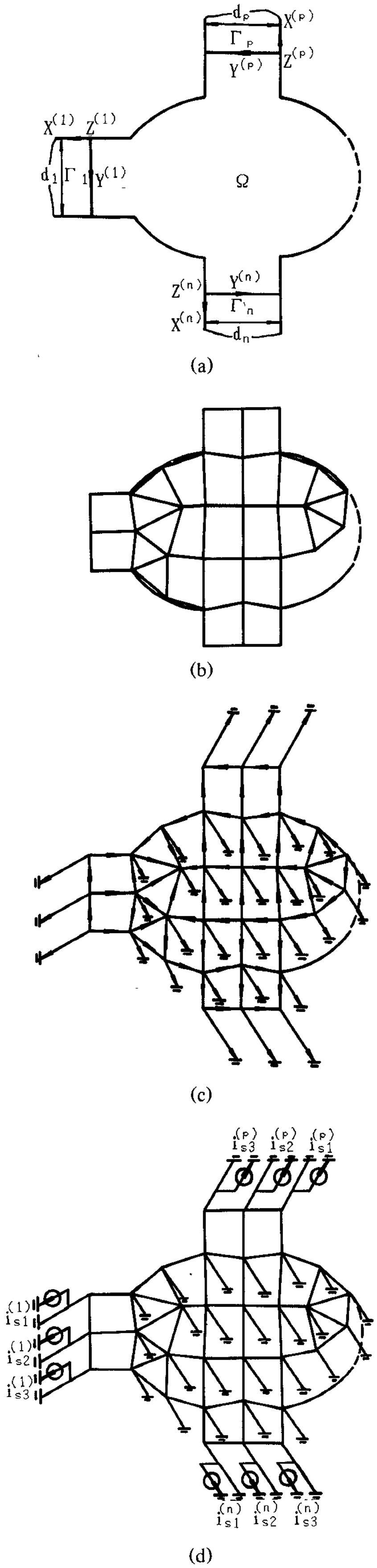

Fig. 1. (a) An arbitrarily shaped waveguide discontinuity. (b) A polygon discretization scheme. (c) The topological model. (d) The network model.

We now introduce a current source i_{sk}, which is defined by

$$a_{kl_0} i_{sk} = -\int_{\overline{n_k q_1}} \frac{\partial \varphi}{\partial n} \, d\Gamma - \int_{\overline{n_k q_{e_k}}} \frac{\partial \varphi}{\partial n} \, d\Gamma. \tag{10}$$

Then (9) may be approximated by

$$\sum_{i=0}^{e_k} a_{kl_i} Y_{k_i} u_{l_i} + a_{kl_0} i_{sk} = \sum_{l=1}^{b} a_{kl} i_{bl} = 0 \tag{11}$$

where

$$Y_{k_0} = -\hat{K}^2 S_k$$

$$Y_{k_i} = \left(\overline{p_{i-1} q_i} + \overline{q_i p_i}\right) / \overline{m_i n_k}, \qquad i = 2,3,\cdots,e_k - 1$$

$$Y_{k_1} = \overline{p_1 q_1} / \overline{m_1 n_k} \quad Y_{ke_k} = \overline{p_{e_k - 1} q_{e_k}} / \overline{m_{e_k} n_k} \tag{12}$$

Introducing the branch current vector $I_b = (i_{b1}, i_{b2}, \cdots, i_{bb})^T$, (7) and (11) can be expressed in matrix form as

$$AI_b = 0 \tag{13}$$

which is a standard form of Kirchhoff's current law.

All current sources introduced above are connected only to the boundary nodes. They may be regarded as the equivalent current sources which replace the effects of the field external to the waveguide discontinuity region Ω. For an E-plane junction, the potential function φ must satisfy the boundary condition $\partial\varphi / \partial n|_{\Gamma_0} = 0$. So we have $i_{sk} = 0$ from (10) for a boundary node on Γ_0. For an H-plane junction we have $\varphi|_{\Gamma_0} = 0$. Hence the boundary nodes on Γ_0 are all grounded and again we have $i_{s_k} = 0$. Therefore only current sources which are connected to the nodes on reference planes are nontrivial.

III. Evaluation of Equivalent Current Sources

Assuming that the dominant TE_{10} mode of unit amplitude is incident from the waveguide q $(q = 1,2,\cdots,n)$, the potential function φ on Γ_p $(p = 1,2,\cdots,n)$ may be expressed as

$$\varphi^{(p)}(x^{(p)}, y^{(p)}) = \sum_{m=1}^{\infty} A_m^{(p)} e^{-j\beta_m^{(p)} x^{(p)}} f_m^{(p)}(y^{(p)}) + \delta_{pq} e^{j\beta_1^{(q)} x^{(q)}} f_1^{(q)}(y^{(q)}) \tag{14}$$

where the normalized basis functions take the form

$$f_m^{(p)}(y^{(p)}) = \left(\frac{\sigma_{m-1}}{b_p}\right)^{1/2} \cos \frac{(m-1)\pi y^{(p)}}{b_p} \tag{15}$$

$$\beta_m^{(p)} = \left\{ K_0^2 \epsilon_{rp} - \left(\frac{\pi}{a_p}\right)^2 - \left[\frac{(m-1)\pi}{b_p}\right]^2 \right\}^{1/2} \tag{16}$$

for an E-plane junction and

$$f_m^{(p)}(y^{(p)}) = \left(\frac{2}{a_p}\right)^{1/2} \sin \frac{m\pi y^{(p)}}{a_p} \tag{17}$$

$$\beta_m^{(p)} = \left[K_0^2 \epsilon_{rp} - \left(\frac{m\pi}{a_p}\right)^2 \right]^{1/2} \tag{18}$$

for an H-plane junction, respectively, and δ_{pq} is the Kronecker δ.

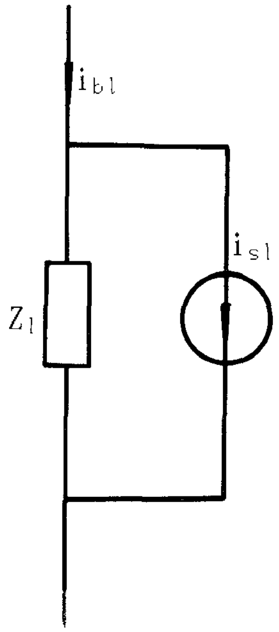

Fig. 2. Standard branch.

Substituting (14) into (10), we obtain

$$i_{sk}^{(p)} = a_{kl_0}\sum_{m=1}^{\infty} j\beta_m^{(p)}A_m^{(p)}I_m^{(p)}(k) - j2\delta_{pq}\beta_1^{(p)}I_1^{(q)}(k) \quad (19)$$

where the expansion coefficients $A_m^{(p)}$ are

$$A_m^{(p)} = \int_0^{d_p}\varphi^{(p)}\left(x^{(p)}=0, y^{(p)}\right) f_m^{(p)}\left(y^{(p)}\right) dy^{(p)}, \qquad m=1,2,\cdots \quad (20)$$

and

$$I_m^{(p)}(k) = \int_{\overline{q_1q_{e_k}}} f_m^{(p)}\left(y^{(p)}\right) dy^{(p)}. \quad (21)$$

From (15) or (17), we have $I_m^{(p)}(k)=O(m^{-1})$ by a direct computation.

Let the number of nodes on Γ_p be denoted by $n^{(p)}$. The potential function $\varphi^{(p)}$ can be approximated by a constant, chosen as $\varphi_k^{(p)}$, over the integration interval $\overline{q_1q_{e_k}}$. Then the expansion coefficients are

$$\begin{aligned} A_m^{(p)} &= \int_0^{d_p}\varphi^{(p)}\left(x^{(p)}=0, y^{(p)}\right) f_m^{(p)}\left(y^{(p)}\right) dy^{(p)} \\ &= \sum_{l=1}^{n^{(p)}} \int_{\overline{q_1q_{e_l}}} \varphi^{(p)}\left(x^{(p)}=0, y^{(p)}\right) f_m^{(p)}\left(y^{(p)}\right) dy^{(p)} \\ &= \sum_{l=1}^{n^{(p)}} \varphi_l^{(p)} I_m^{(p)}(l) \qquad (m=1,2,\cdots). \end{aligned} \quad (22)$$

Introducing the above expression into (19), we obtain

$$i_{sk}^{(p)} = \sum_{l=1}^{n^{(p)}} a_{lk}^{(p)}\varphi_l^{(p)} - j2\delta_{pq}\beta_1^{(q)}I_1^{(q)}(k) \quad (23)$$

where

$$a_{lk}^{(p)} = a_{kl_0}\sum_{m=1}^{\infty} j\beta_m^{(p)} I_m^{(p)}(l) I_m^{(p)}(k). \quad (24)$$

A system of algebraic equations may be obtained by letting $k=1,2,\cdots,n^{(p)}$ successively in (23), which can then be expressed in matrix form as

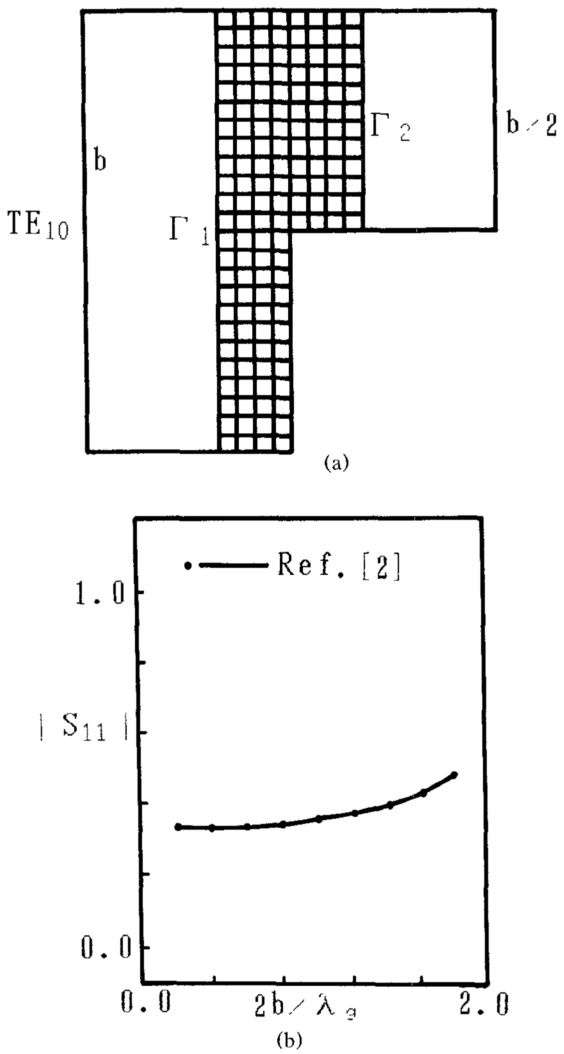

Fig. 3. (a) An E-plane step and its discretization scheme. (b) Magnitude of reflection coefficient.

$$I^{(p)} = A^{(p)}V^{(p)} + C^{(p)} \quad (25)$$

where $A^{(p)} = \{a_{ij}^{(p)}\}$. $I^{(p)} = (i_{s1}^{(p)}, i_{s2}^{(p)}, \cdots, i_{sn^{(p)}}^{(p)})^T$, and $V^{(p)} = (\varphi_1^{(p)}, \varphi_2^{(p)}, \cdots, \varphi_{n^{(p)}}^{(p)})^T$ are the current source vector and the node-to-datum voltage vector on Γ_p respectively. $C^{(p)} = -j2\delta_{pq}\beta_1^{(q)}(I_1^{(q)}(1), I_1^{(q)}(2), \cdots, I_1^{(q)}(n^{(p)}))^T$ will be referred to as the excitation vector on $\Gamma^{(p)}$.

IV. Diakoptics

The standard branch of the network model is shown in Fig. 2. The branch relation may be expressed as

$$\begin{cases} I_b = YU_b + I_s \\ U_b = Z(I_b - I_s) \end{cases} \quad (26)$$

where $Z=\mathrm{diag}(Z_1, Z_2, \cdots, Z_b)$ and $Y=\mathrm{diag}(Y_1, Y_2, \cdots, Y_b)$ are branch impedance and admittance matrix respectively, and $I_s = (i_{s1}, i_{s2}, \cdots, i_{sb})^T$ is the current source vector. Following the standard procedure described in [1], we obtain the diakoptic

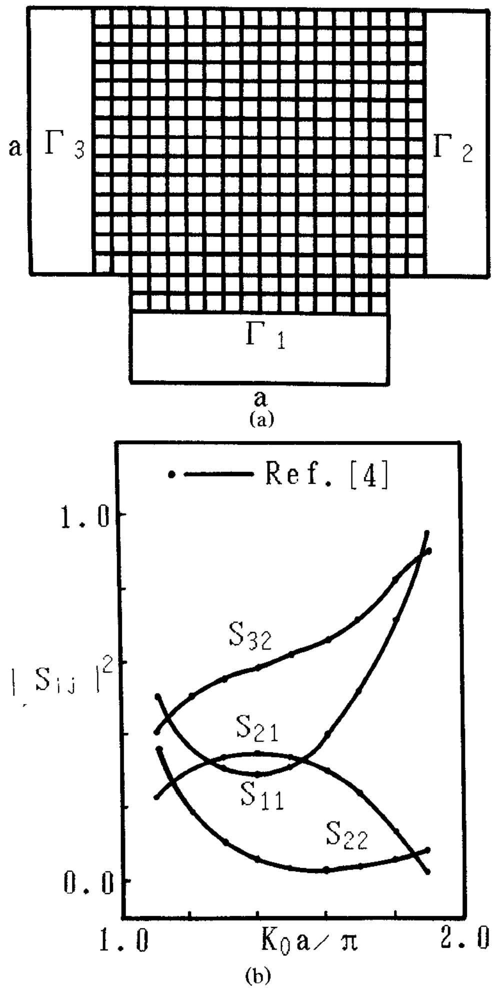

Fig. 4. A T junction and its discretization scheme. (b) Power reflection and transmission coefficients of the T junction.

node equation as follows:

$$Y_{ni}V_i + A_{li}I_b^t = -A_{ri}I_{si}^r, \qquad i = 1, 2, \cdots, K$$

$$\sum_{i=1}^{K} A_{ti}^T V_i - Z_t I_b^t = 0 \tag{27}$$

where $Y_{ni} = A_{ri}Y_{ri}A_{ri}^T$; A_{ri}, Y_{ri}, V_i, and I_{si}^r are the reduced incidence matrix, branch admittance matrix, node-to-datum voltage vector, and current source vector of the ith component part GR_i; and A_{ti} is the reduced incidence matrix of GR_t with the tearing branches.

Assuming that all boundary nodes on Γ_p are inside part GR_i and the remaining nodes of GR_i are either inside Ω or on Γ_0. Then the vector V_i can be decomposed into the form $V_i = ((V^{(p)})^T, V_I^T)^T$. If the numbering of the branches containing the current sources is from $b_i(1)$ to $b_i(n^{(p)})$, then the current source vector I_{si}^r can be expressed in the form

$$I_{si}^r = \left.\begin{bmatrix} 0 \\ I^{(p)} \\ 0 \end{bmatrix}\right\} \begin{matrix} b(1) \\ \vdots \\ b_i(n^{(p)}) \end{matrix} = \begin{bmatrix} 0 & 0 \\ A^{(p)} & 0 \\ 0 & 0 \end{bmatrix} \begin{bmatrix} V^{(p)} \\ V_I \end{bmatrix} + \begin{bmatrix} 0 \\ C^{(p)} \\ 0 \end{bmatrix} = A_i^r V_i + C_i \tag{28}$$

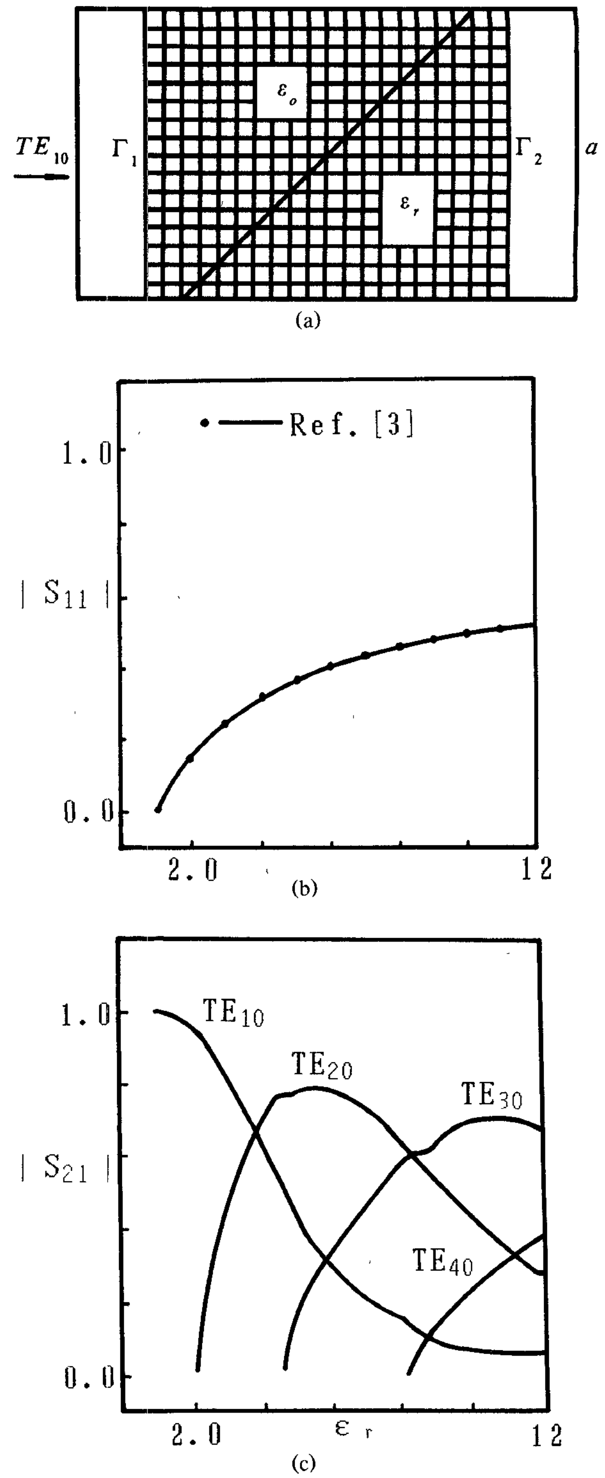

Fig. 5. (a) An inhomogeneous junction and its discretization. (b) Magnitude of reflection coefficient. (c) Magnitude of transmission coefficients.

from (25). Substituting the above expression into (27), we obtain

$$\left\{ Z_t + \sum_{i=1}^{K} A_{ti}^T [Y_{ni} + A_{ri}A_i^r]^{-1} A_{ti} \right\} I_b^t = -\sum_{i=1}^{K} A_{ti}^T [Y_{ni} + A_{ri}A_i^r]^{-1} A_{ri} C_i \tag{29}$$

from which the tearing branch current I_b^t can be determined.

The node-to-datum voltage vector V_t can then be found by using the relation

$$V_t = -\left[Y_{nt} + A_{rt}A_t^r\right]^{-1}\left[A_{rt}C_t + A_{tt}I_b^t\right]. \tag{30}$$

The solutions of φ on Γ_p allow the determination of the scattering parameter S_{ij} of the TE_{10} mode as follows:

$$S_{pp} = \int_0^{d_p} \varphi^{(p)}\left(x^{(p)} = 0, y^{(p)}\right) f_1^{(p)}\left(y^{(p)}\right) dy^{(p)} - 1 \tag{31}$$

$$S_{pq} = \left(\frac{\beta_1^{(p)}\hat{\epsilon}_{rq}}{\beta_1^{(q)}\hat{\epsilon}_{rp}}\right)^{1/2} \int_0^{d_p} \varphi\left(x^{(p)} = 0, y^{(p)}\right) f_1^{(p)}\left(y^{(p)}\right) dy^{(p)} \tag{32}$$

In (32), both $\hat{\epsilon}_{rp}$ and $\hat{\epsilon}_{rq}$ should be replaced by 1 for H-plane junctions.

V. Numerical Results

To demonstrate the validity and effectiveness of the method, computed results for various H- and E-plane waveguide discontinuities have been obtained and compared with other theories available. In the analysis, the first six evanescent higher order modes are used in (24).

Numerical results for two-port and multiport junctions are given in Figs. 3 and 4. The NMD method is applicable to the analysis of multimedia problems and can also be easily applied to the frequency range in which waveguide propagates multimodes. Fig. 5(a) shows an inhomogeneous junction and its discretization scheme. In this case the boundary conditions $\varphi_{\text{air}} = \varphi_{\text{dielectric}}$ and $\partial\varphi/\partial n|_{\text{air}} = -\partial\varphi/\partial n|_{\text{dielectric}}$ should be taken into account on the interface between air and dielectric. Fig. 5(b) shows the results of the magnitude of reflection coefficient obtained by the NMD method and the moment method [3], respectively, and good agreement is obtained. The NMD results of the transmission coefficients given by Fig. 5(c) are quite different from those of the moment method [3]. In the moment method, the transmission coefficients of the higher order modes are not zero at the cutoff values of ϵ_r. As a check on the accuracy of our solutions, the total power sums P_i^s have been evaluated and the power conservation condition is satisfied to an accuracy of $\pm 10^{-5}$. So the results given by the NMD method are convincing.

VI. Conclusion

In this paper a network model decomposition algorithm has been developed which permits the scattering matrices to be computed for arbitrarily shaped H- or E-plane junctions. Computed results for various H- and E-plane junctions are also given as a demonstration of the validity of the method. Our discussions and results obtained indicate that the network model decomposition method has the virtues of simplicity and generality, and so is a powerful tool for the analysis of waveguide discontinuity problems.

References

[1] Wen Geyi, "Numerical solution of transmission line problems by a network model decomposition method based on polygon discretization," *IEEE Trans. Microwave Theory Tech.*, vol. 38, pp. 1086–1091, Aug. 1990.

[2] N. Marcuvitz, *Waveguide Handbook*. New York: McGraw-Hill, 1951.

[3] Y. L. Chow and S. C. Wu, "A moment method with mixed basis functions for scattering by waveguide junctions," *IEEE Trans. Microwave Theory Tech.*, vol. MTT-21, pp 333–340, July 1973.

[4] M. Koshiba and M. Suzuki, "Applications of the boundary element method to waveguide discontinuities," *IEEE Trans. Microwave Theory Tech.*, vol. MTT-34, pp. 301–307, 1986.

Analysis of $E-H$ Plane Tee Junction Using a Variational Formulation

B. N. Das and N. V. S. Narasimha Sarma

Abstract —**An analysis of an $E-H$ plane tee junction taking the width of the slot and wall thickness into account is presented. The parameters of the three-port equivalent network are determined. The reflection as well as transmission parameters are evaluated. A comparison between theoretical and experimental results is presented.**

I. Introduction

In the investigations on $E-H$ plane T junctions reported in the literature [1], the internal energy storage required for the evaluation of impedance loading has been found by regarding the coupling slot as a superposition of transverse and longitudinal components. Hsu and Chen [2] have presented a method of analysis which is not based on this concept. In the coordinate transformation they use, there is no scope for taking the effect of slot width into account. Further, in [2, eq. (8)] limits of integration were not properly taken. In the method suggested by Stevenson [3] and used by Elliott *et al.* [4] the expression involves a singularity, which, it is suggested, should be avoided for better accuracy. But the method for avoiding the singularity is not indicated.

In the present work, a three-port equivalent network for an $E-H$ plane tee junction is determined taking into account the effect of waveguide wall thickness and considering the contribution of the dominant mode to the imaginary part of the self-reaction.

From a knowledge of the equivalent network parameters, the net impedance loading, reflection coefficient, and coupling are evaluated for an $E-H$ plane tee junction. A comparison between theoretical and experimental results is also presented.

II. Analysis

The inclined slot-coupled $E-H$ plane tee junction together with the coordinate system is shown in Fig. 1. The three-port equivalent circuit of the junction is shown in Fig. 2. For a matched termination at port 3, the variational expression for the

Manuscript received September 26, 1990; revised April 3, 1991.

B. N. Das is with the Department of Electronics and Electrical Communication Engineering, Indian Institute of Technology, Kharagpur, 721 302 India.

N. V. S. Narasimha Sarma is with the Department of Electronics and Computer Science, Regional Engineering College, Warangal, 506 004 India.

IEEE Log Number 9102332.